# ATOMISTIC SIMULATION OF DISLOCATION GENERATION AT SURFACE STEPS IN METALS AND SILICON

S. Brochard, J. Godet, L. Pizzagalli, P. Beauchamp
*Laboratoire de Métallurgie Physique, UMR 6630 Université de Poitiers-CNRS, SP2MI, BP 30179, Futuroscope Chasseneuil Cedex, France*

**Abstract**      Atomic scale simulations of a crystal with a free surface containing a surface step, submitted to a uniaxial stress have been performed using semi-empirical potentials representing metals (aluminum and copper) and silicon. In metals, different types of dislocations are nucleated for stresses well below the theoretical strength, according to the stress orientation, and the nucleation is preceded by a localization of shear confined into a single dense plane in-zone with the step. As expected, the behavior in silicon is very different from that of metals: besides complex plastic deformations appearing for large stresses, for those orientations where it has been possible to form dislocations, they have been found to glide in the shuffle set.

**Keywords**      Dislocation nucleation; Atomistic simulations; Surface and interface

## 1.      INTRODUCTION

In nanostructures (thin films, nanograins...), the observed presence of dislocations cannot be explained by the Frank-Read source mechanism because of the reduced dimensions and / or the absence of pre-existing dislocation to activate the source. In such materials, the interface or surface defects, such as steps, are good candidates to act as dislocation sources.

The mechanism of dislocation nucleation from a surface step being still out of reach of experiments, atomic scale simulations are expected to bring useful information. We have performed atomistic calculations of dislocation generation from a surface step under external applied stress. The first studies were conducted in metals, for which reliable interatomic potentials, well adapted for simulations at this length scale, exist. Afterwards, we studied silicon, as it is a prototype of semiconductor materials used in microelectronic devices, where the mechanisms under study are expected to occur frequently.

The main geometrical difference between the diamond-like structure of silicon and the simple f.c.c. crystals lies in the presence of two atoms per unit cell in the diamond-like structure, yielding two kinds of {111} plane sets, namely the shuffle set and the glide set [1].

In silicon it is commonly accepted that, at least at high temperature, plastic deformation is mediated through dissociated dislocations located in glide set planes [2]. At low temperature, plastic deformation requires specific deformation conditions, as for example a confining pressure, to avoid fracture of the material. During recent experiments at low temperature perfect dislocations have been observed [3], which is consistent with gliding in the shuffle set plane, as predicted by calculations of the generalized stacking fault energies [4, 5, 6, 7]. In the study presented here, a particular attention will be paid to the type of plane, shuffle or glide, where the dislocations are nucleated in silicon, when they are.

## 2. MODEL

In this section, we briefly present the geometry and computational method used for this work. More detailed information can be found in references [8, 9]

## 2.1 Geometry – application of stress

In order to study the dislocation nucleation from a surface step, a crystal limited by a {100} free surface is constructed. In all the calculations presented here, the bulk crystal is simulated by freezing the opposite face; it has been ensured that releasing this constraint does not change the kind of dislocation nucleated, nor in a significant way the critical stress for dislocation nucleation. In the surface plane, the step lies along a <110> dense direction, intersection of a {111} glide plane and the surface. For the f.c.c. metals, this orientation determines in a unique way the resulting monoatomic step. In silicon, because of the 2×1 surface reconstruction, and depending if a single or a double step is considered, four different steps can result from this orientation [10]. The most stable step configurations ($S_A$ and $D_B$) have been studied, but systematic calculations have been conducted only for $D_B$ steps, which step height corresponds to the Burgers vector of a perfect dislocation. In this configuration, the step line is parallel to the dimerization direction (figure 1).
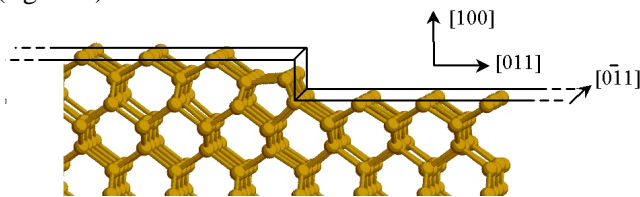


*Figure -1.* Orientation and geometry of the slab for silicon.

The uniaxial stress, whose orientation is contained in the surface plane, is applied through the displacements of all the atoms. These displacements are calculated using linear anisotropic elasticity (the elastic constants being determined for each potential). Both tensile and compressive stresses are studied. After the application of stress, the simulated box dimensions are maintained via two fixed buffers or through periodic boundary conditions along the direction perpendicular to the step line (in the latter case, two opposite steps are introduced on the surface). Along the step line direction, periodic boundary conditions are applied, with enough thickness to prevent spurious interaction between an atom and its image. However, the thickness along this direction, which is also the dislocation line direction when dislocations are nucleated, is too small to allow the formation of a half-loop: the nucleated dislocations are always straight. Different stress orientations have been studied. The stress direction is indicated by $\alpha$ (figure 2), the angle between the normal to the step line and the stress direction ($\alpha = 0°$ corresponds to a stress orientation normal to the step line).
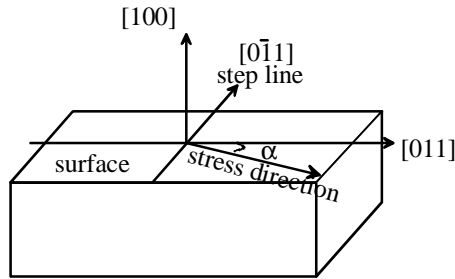


*Figure -2.* Geometry of the studied system.

## 2.2    Algorithms – potentials

For metals, simulations at 0 K were done, using a conjugate gradient algorithm for relaxation. For silicon, both relaxation at 0 K and molecular dynamics (MD) simulation [11] at finite temperature (300 K) have been performed, in order to favor dislocation nucleation. The MD simulation lasted typically 50 ps, and was then followed by a quench to minimize the energy. In all cases, the minimum energy was assumed to be reached when the mean force on each atom was less than $10^{-7}$ eV/Å. The interatomic interactions are derived from semi-empirical many-body potentials for the metals studied here (aluminum and copper) [12]. For silicon, we used three potentials that have proved their efficiency in different contexts, namely Stillinger-Weber potential (SW) [13], Tersoff potential (T) [14] and EDIP (Environment-Dependent Interatomic Potential) [15].

## 3.     METALS (ALUMINUM AND COPPER)

Two different f.c.c. metals, aluminum and copper, have been studied. They differ in both their intrinsic stacking fault energy and elastic anisotropy coefficient, so that different behaviors are expected. With the potentials used, the intrinsic stacking fault energy for aluminum is 155 mJ/m$^2$ and the anisotropy factor is 1.07; for copper the values are 29 mJ/m$^2$ and 3.15. In the following, the results on metals are briefly described, emphasizing the main points for later comparison with the more complicated case of silicon. More details on metals can be found in [8, 16].

### 3.1     Results

The results for metals are summarized in Table 1, together with the type of leading and trailing dislocations resulting from the stacking of {111} planes, the Schmid factors on these dislocations, and the theoretical shear strengths. The stress orientations have been chosen so that the ratio between Schmid factors on the trailing and leading dislocations is 0.5 or 2 ($\alpha = 0°$ and $\alpha = 45°$) and 1 ($\alpha = 18°$). The main results are:

(i) The dislocations are almost always formed at the step, and then glide in {111} planes in-zone with the step.

(ii) When the nucleation event originates from the step, the stress threshold for dislocation nucleation is well below the theoretical shear strength.

(iii) Except in few cases where technical constraints can be put forward, the type of dislocation formed is well explained by the stress orientation (see the Schmid factors) and the stacking of the {111} planes. For example, for $\alpha = 0°$, 90° Shockley partial dislocations are nucleated in traction, since they have the largest Schmid factor, and intrinsic stacking faults remain in the crystal after their formation. On the contrary, for the same orientation but in compression, the leading dislocation must be a 30° Shockley (a 90° would involve a prohibited stacking of the type ...ABCAABC...). But the Schmid factor on this partial dislocation is half the one for 90° Shockley, and no dislocation is nucleated until the theoretical strength is reached (aluminum) or a perfect 60° dislocation is nucleated for a quite large stress (copper).

(iv) Although some differences can be noted, the stress thresholds and the type of defect formed in relation with the stress orientation, are comparable in aluminum and copper.

*Table -1.* Dislocations nucleated in aluminum and copper with the corresponding strain and stress. The type of leading and trailing partial dislocations, as well as the corresponding Schmid factors are indicated in the first column. The value of the theoretical shear strength is given for a stress orientation normal to the step line.

| | aluminum | copper |
|---|---|---|
| **theoretical shear strength** | 13.7% (10.6 GPa) | 7.3% (10.6 GPa) |
| $\alpha = 0°$, **traction** <br> leading: 90° $\left(\sqrt{2}/3\right)$ <br> trailing: 30° $\left(\sqrt{2}/6\right)$ | two 90° Shockley partial dislocations at the step <br> $\varepsilon = 8.4\%$ ($\sigma = 6.5$ GPa) | one 90° Shockley partial dislocation at the step <br> $\varepsilon = 5.1\%$ ($\sigma = 7.4$ GPa) |
| $\alpha = 0°$, **compression** <br> leading: 30° $\left(\sqrt{2}/6\right)$ <br> trailing: 90° $\left(\sqrt{2}/3\right)$ | surface and bulk nucleation <br> $\varepsilon = 13.0\%$ ($\sigma = 10$ GPa) | one perfect 60° dislocation and one 30° Shockley partial at the step <br> $\varepsilon = 6.6\%$ ($\sigma = 9.6$ GPa) |
| $\alpha = 18°$, **traction** <br> leading: 90° $\left(9\sqrt{2}/30\right)$ <br> trailing: 30° $\left(9\sqrt{2}/30\right)$ | one perfect 60° dislocation at the step <br> $\varepsilon = 9.5\%$ ($\sigma = 7$ GPa) | one 90° Shockley partial dislocation at the step <br> $\varepsilon = 6\%$ ($\sigma = 6.5$ GPa) |
| $\alpha = 18°$, **compression** <br> leading: 30° $\left(9\sqrt{2}/30\right)$ <br> trailing: 90° $\left(9\sqrt{2}/30\right)$ | one perfect 60° dislocation at the step <br> $\varepsilon = 9.5\%$ ($\sigma = 7$ GPa) | one perfect 60° dislocation at the step and one 30° Shockley partial at the surface <br> $\varepsilon = 7.7\%$ ($\sigma = 8.5$ GPa) |
| $\alpha = 45°$, **traction** <br> leading: 90° $\left(\sqrt{2}/6\right)$ <br> trailing: 30° $\left(\sqrt{2}/3\right)$ | one perfect 60° dislocation at the step <br> $\varepsilon = 11\%$ ($\sigma = 8$ GPa) | — |
| $\alpha = 45°$, **compression** <br> leading: 30° $\left(\sqrt{2}/3\right)$ <br> trailing: 90° $\left(\sqrt{2}/6\right)$ | three 30° Shockley partial dislocations at the step <br> $\varepsilon = 9.5\%$ ($\sigma = 7$ GPa) | — |

## 3.2   Localized shear prior to dislocation nucleation

An important result of the calculations on metals is the presence, prior to any dislocation generation, of a shear localized in the {111} glide plane where the first nucleation event will occur [16]. It has been shown that this localized shear is a precursor of the fully formed dislocation, the latter appearing when the shear reaches, locally, a critical value for which the crystal becomes mechanically unstable (the theoretical shear strength in Frenkel model [17]). This shear localization has been related, via a non linear tension-shear coupling, to the local stress field originating from the step when an external stress is applied. It may be worth seeking if such a localized shear appears in silicon, as in metals.

## 4. SILICON

As mentioned in section 2, three different potentials were used to perform the calculations in silicon. In subsection 4.1 a comparative study of the three potentials is presented. Then, in subsection 4.2, we detail the results obtained with the SW potential, which proved to be the best suited for the problem studied here.

## 4.1 Comparative study of Si potentials

Preliminary tests indicated that the defects formed in strained samples were dependent on the potential used. In order to discriminate between the three potentials, their shear properties have been confronted to ab initio calculations. Two different types of tests have been conducted, the first involving homogeneous shear on {111} planes, and the second, generalized stacking fault energy surfaces ("γ-surfaces", as named by Vitek [18]) calculations on these planes. The criterion of choice for the potential is based on the description of the mechanism and energetics of bond switching which necessarily occurs at large enough strain.

The study of large homogeneous shear properties, in addition to more generally considered γ-surfaces, was partly motivated by the observation of a rather homogeneous strain field, even in the step region (absence of localized shear) in the case of silicon [9]. The results obtained with the three empirical potentials and an ab initio simulation [19] are detailed elsewhere [20]. They all agree on that, when the imposed shear is large, the mechanism of neighbor switching occurs by breaking the bonds across the shuffle set. In glide set planes, the deformation remains elastic, depending almost linearly on the internal shear stress. But the main point is that only the SW potential shows smooth energy variations and continuous internal shear stress, close to what is obtained with ab initio.

Subsequently, γ-surfaces have been computed for the three empirical potentials, and compared to first-principles results [4, 6]. Tersoff and EDIP potentials yield unstable stacking fault energy values closer to ab initio than the SW potential [20], but they show discontinuities that are not obtained with the SW potential, nor with ab initio techniques. This is particularly obvious on the curves derived from the γ-surfaces in the directions corresponding to a perfect 60° dislocation (<110>) in the shuffle or the glide plane or a partial Shockley dislocation (<112>) in the glide plane, where the continuity and smoothness of the ab initio curves are reproduced only by the SW potential, and not by Tersoff and EDIP potentials.

Consequently, the best potential for the problem studied here, that is formation of plastic defects under large stress, is clearly the SW potential.

## 4.2 Survey of the results with the SW potential

The results obtained with the SW potential are summarized in Table 2. Here again, different stress directions have been analyzed, favoring orientations for which the Schmid factor is maximum on the 90° Shockley partial dislocation ($\alpha = 0°$), on the 60° perfect dislocation ($\alpha = 22.5°$), or on the screw dislocation ($\alpha = 45°$).

*Table -2.* Type of dislocations nucleated in silicon and corresponding strain. The type of leading and trailing partial dislocations, as well as the corresponding Schmid factors are indicated in the first column. The value of the theoretical shear strength is given for a stress orientation normal to the step line.

| | T = 0 K | T = 300 K |
|---|---|---|
| **theoretical shear strength** | 32% (48 GPa) | — |
| $\alpha = 0°$, **traction** <br> leading: 90° $\left(\sqrt{2}/3\right)$ <br> trailing: 30° $\left(\sqrt{2}/6\right)$ | fracture <br> $\varepsilon = 25.1\%$ | fracture <br> $\varepsilon = 13.1\%$ |
| $\alpha = 0°$, **compression** <br> leading: 30° $\left(\sqrt{2}/6\right)$ <br> trailing: 90° $\left(\sqrt{2}/3\right)$ | formation of a microtwin at the step <br> $\varepsilon = 7.8\%$ | — |
| $\alpha = 22.5°$, **traction** <br> leading: 90° (0.40) <br> trailing: 30° (0.44) | one perfect 60° dislocation at the step <br> $\varepsilon = 18.7\%$ | perfect 60° dislocations at the step <br> $\varepsilon = 12.5\%$ |
| $\alpha = 22.5°$, **compression** <br> leading: 30° (0.44) <br> trailing: 90° (0.40) | plastic deformation in {111} planes <br> $\varepsilon = 10\%$ | one perfect 60° dislocation at the step <br> $\varepsilon = 7.5\%$ |
| $\alpha = 45°$, **traction** <br> leading: 90° $\left(\sqrt{2}/6\right)$ <br> trailing: 30° $\left(\sqrt{2}/3\right)$ | formation of microtwins from surface and bulk <br> $\varepsilon = 19.7\%$ | — |
| $\alpha = 45°$, **compression** <br> leading: 30° $\left(\sqrt{2}/3\right)$ <br> trailing: 90° $\left(\sqrt{2}/6\right)$ | one perfect 60° dislocation at the step <br> $\varepsilon = 14.0\%$ | — |

It must be pointed out first that for all orientations, and at 0 K as well as at 300 K, the plastic defects (dislocations, microtwins or more complicated defects) are nucleated and glide in {111} planes of the shuffle set.

It may then be noticed that dislocation nucleation is in general much more difficult than in metals, which is consistent with the high theoretical shear strength. Another characteristic is that the defects are more easily formed in compression than in traction, in the sense of lower critical deformations. Complementary studies are needed to clarify this point. For all stress orientations, the presence of the step and temperature reduce the yield

stress, but the type of defect formed is not as easily rationalized as in the case of f.c.c. metals. Except for the microtwins, which are a feature of the SW potential, the defects formed are perfect 60° dislocations.

As a rule of thumb, dislocations are not nucleated in glide set planes for the relatively low temperatures studied here, in agreement with the usual explanation that it would involve the breaking of three covalent bonds (compared to only one in the shuffle set planes). As a result, 90° Shockley partial dislocations (for $\alpha = 0°$ in traction) or 30° Shockley (for $\alpha = 45°$ in compression), which necessarily belong to a glide set plane (figure 3), are not nucleated, contrary to what happens in metals. For these stress orientations, in silicon, the applied deformation is accommodated via the propagation of a crack approximately normal to the surface for $\alpha = 0°$ in traction, and via the nucleation of a perfect 60° dislocation for $\alpha = 45°$ in compression.
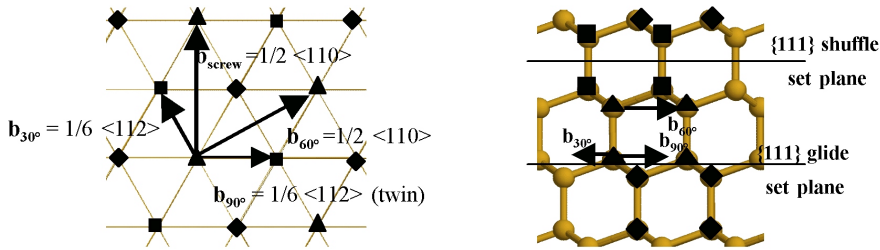


*Figure -3.* Diamond-like structure with the different Burgers vectors projected along <111> (left) and along <110> (right).

Regarding the two cases for which the trailing partial dislocations are favored by the Schmid factor against perfect dislocations or against the leading partial dislocations, i.e. $\alpha = 0°$ in compression and $\alpha = 45°$ in traction, a particular type of microtwin has been obtained and found to be formed by glide events occurring in the shuffle set [21]. Once again, it is the impossibility of nucleating partial dislocations which leads to the formation of this probably unphysical plastic deformation.

Finally, for $\alpha = 22.5°$, perfect 60° dislocations are nucleated (figure 4), as expected, both in traction and in compression, and more easily with temperature than without. As a matter of fact, at 0 K in compression, no dislocation forms at the step, and plastic events hardly analyzable, but clearly originating from the step in {111} planes are obtained. In traction the applied deformation must be increased up to 18.7% before the perfect dislocation forms from the step.

An important point of these calculations is that the active planes for gliding are always {111} planes of the shuffle set, a result also obtained with the other potentials (Tersoff and EDIP). The difficulty of breaking bonds

seems to be a determinant factor in the process of dislocation nucleation in this covalent material.
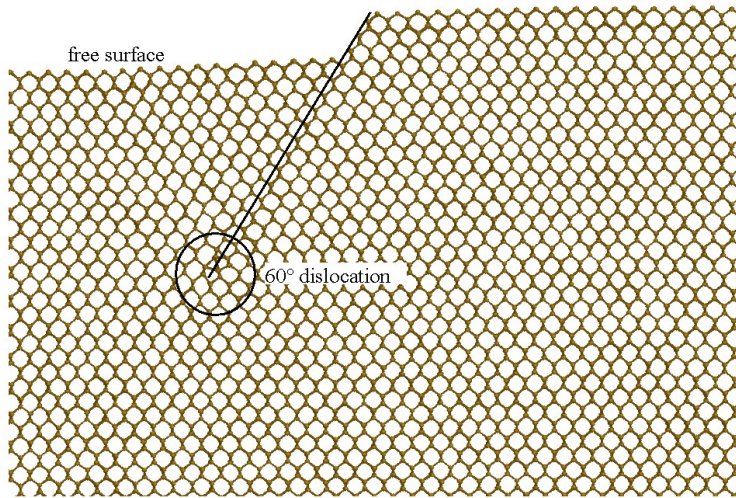


*Figure -4.* 60° dislocation nucleated for $\alpha = 22.5°$ and for an applied compression strain of 7.5% at 300 K. The solid line indicates the shuffle set plane where the dislocation has glided.

Furthermore, as mentioned previously, no precursory shear in the {111} glide planes in zone with the step is observed. An analysis based on a point force model has proved that the non-appearance of a localized shear is not due to the step geometry [9]. The non-appearance of the shear localization backs up once again the idea of a predominant role of the hard bond breaking in silicon.

## 5. CONCLUSION

Calculations of dislocation formation from an atomic surface step in a stressed crystal have been performed. Two f.c.c. metals, aluminum and copper, and a model semiconductor, silicon, have been studied. In both cases, the uniaxial stress orientation acts directly on the type of defect formed. But as expected, a different behavior is observed between metals and silicon. In silicon, dislocation formation is more difficult and requires higher stress. Perfect dislocations form in the shuffle set, and partial dislocations are never nucleated, which is quite different from what occurs in metals. In order to understand the mechanism of dislocation nucleation, the crystal structure just before nucleation has been analyzed. In metals, a localized shear in the glide plane where the first nucleation event will occur

is observed, which is not the case in silicon. The localized shear observed in metals has been analyzed in terms of a tension-shear coupling [16]. Such a coupling must play a determinant role in the mechanism of dislocation nucleation, as suggested by previous studies [22], and may be different for a covalent bond across a shuffle set plane and a metallic bond.

For the particular case of silicon, the plastic deformations observed at the low temperatures studied here always occur in shuffle set planes. Nevertheless, the results for very high deformations depend on the type of empirical potential used. A comparative study between three potentials and ab initio calculations has proved that the SW potential is the best suited for the problem under study here. However, it would be safer to check the results obtained with the SW potential by performing an ab initio simulation of the whole mechanism of dislocation nucleation at a surface step. The feasibility of such a calculation is under consideration at present.

### References

[1] Hirth J.P., Lothe J., *Theory of Dislocations* (New York, Wiley), 1982

[2] Alexander H., *Dislocations in Solids*, vol. 7, edited by F.R.N. Nabarro (Amsterdam: North-Holland), 1986

[3] Rabier J., Cordier P., Demenet J.L., Garem H., *Materials Science & Engineering* **A309-310** (2001) 74

[4] Kaxiras E., Duesbery M.S., *Physical Review Letters* **70** (1993) 3752

[5] Joós B., Ren Q. and Duesbery M.S., *Physical Review B* **50** (1994) 5890

[6] Juan Y.M. and Kaxiras E., *Philosophical Magazine. A* **74** (1996) 1367

[7] Miyata M. and Fujiwara T., *Physical Review B* **63** (2001) 045206

[8] Brochard S., Beauchamp P., Grilhé J., *Philosophical Magazine A* **80** (2000) 503

[9] Godet J., Pizzagalli L., Brochard S., Beauchamp P., *Scripta Materialia* **47** (2002) 481

[10] Chadi D.J., *Physical Review Letters* **59** (1987) 1691

[11] XMD code, written by Rifkin J. (URL: http://www.ims.uconn.edu/centers/simul#Software)

[12] Aslanides A., Pontikis V., *Computational Materials Science* **10** (1998) 401

[13] Stillinger F.H., Weber T.A., *Physical Review B* **31** (1985) 5262

[14] Tersoff J., *Physical Review B* **38** (1988) 9902

[15] Bazant M.Z., Kaxiras E., *Physical Review B* **56** (1997) 8542

[16] Brochard S., Beauchamp P., Grilhé J., *Physical Review B* **61** (2000) 8707

[17] Frenkel J., *Z. Physik* **37** (1926) 572

[18] Vitek V., *Philosophical Magazine* **18** (1968) 773

[19] The ABINIT code is a common project of the Université Catholique de Louvain, Corning Incorporated and other contributors (URL: http://www.abinit.org)

[20] Godet J. et al., submitted to *Journal of Physics: Condensed Matter*

[21] Godet J., Pizzagalli L. Brochard S., Beauchamp P., to be published in 12th Computational Materials Science workshop (2002) proceedings

[22] Sun Y., Beltz G.E., Rice J.R., *Materials Science & Engineering* **A170** (1993) 67